Available online at www.sciencedirect.com
ScienceDirect
Trans. Nonferrous Met. Soc. China 25(2015) 3181−3188
Transactions of Nonferrous Metals Society of China
www.tnmsc.cn

Densification process of 10%B_4C−AA2024 matrix composite strips by semi-solid powder rolling

Zhuo-qiang MO, Yun-zhong LIU, Hui-fang JIA, Min WU

National Engineering Research Center of Near-net-shape Forming for Metallic Materials, South China University of Technology, Guangzhou 510640, China

Received 21 November 2014; accepted 10 March 2015

Abstract: Semi-solid powder rolling (SSPR) is a novel strip manufacturing process, which includes the features of semi-solid rolling and powder rolling. In this work, densification process and deformation mechanisms of B_4C and AA2024 mixed powders in the presence of liquid phase were investigated. The relationships between relative densities and rolling forces were analyzed as well. The results show that liquid fraction plays an important role in the densification process which can be divided into three stages. Rolling deformation is the main densification mechanism in deformation area when the liquid fraction is lower than 20%. When the liquid fraction is equal to or higher than 20%, the flowing and filling of liquid phase are the densification mechanisms in deformation area. The relative densities increase with increasing rolling forces. The relative density–rolling force curves are similar at 550 °C and 585 °C. The characteristics of the curve shapes are apparently different at 605 °C and 625 °C.

Key words: semi-solid powder rolling; composite strip; densification process; rolling deformation

1 Introduction

Aluminum metal matrix composites (Al MMCs) emerge as advanced engineering materials due to their high strength, high specific modulus and low coefficient of thermal expansion [1]. The intrinsic properties of B_4C such as lightweight (only 2.52 g/cm^3), good wear resistance (second only to diamond) as well as neutron absorbing ability make it have important applications in many fields. For example, B_4C−AA6061 metal matrix composites have been used as an excellent neutron absorber material in the nuclear industry [2,3]. Strip products are usually manufactured by conventional ingot metallurgy. Subsequently, the materials are further processed (e.g., heat treatment, cold or hot rolling) to meet the required properties. So, the production run is long and energy wasting. The composite strip prepared by conventional ingot metallurgy also has its own drawbacks such as non-uniform distribution of the reinforcement and undesirable chemical reaction. Based on the above, a novel manufacturing process was proposed for metal strip termed “semi-solid powder rolling (SSPR)”, which includes some advantages of semi-solid processing (SSP) and powder metallurgy (PM). The authors have successfully prepared AA7050 aluminum alloy strips with superior properties by this process, and a factor of progress remarkability (F) was proposed and calculated to discuss the relationship between deformation and densification [4].

It is well known that the properties of composite are mainly determined by the microstructure, relative density and the particle distribution. ATKINSON and LIU [5] studied coarsening rate of microstructure in semi-solid aluminium alloys, and the result shows that extensive coarsening will have a deleterious effect on the final mechanical properties. Literatures survey on densification behavior of composite powder is scarce, especially the powders in semi-solid state. LANGE et al [6] studied the densification behavior of mixed powders under various types of powders and experimental conditions by powder metallurgy. WU and KIM [7] studied the compaction behavior of Al6061 powders and discussed the relationship between the compaction pressure and relative density of powder in the semi-solid state. KIM et al [8] studied the densification behavior of mixed powder under cold compaction. BORSA et al [9] studied liquid phase

Foundation item: Project (2013KJCX0014) supported by the Key Project of Department of Education of Guangdong Province, China
Corresponding author: Yun-zhong LIU; Tel: +86-20-87110099; E-mail: yzhliu@scut.edu.cn
DOI: 10.1016/S1003-6326(15)63950-4

sintering (LPS) of Al_2O_3/SiC nanocomposites, and discussed the densification behavior in detail.

Even though the densification behaviors of composite during hot extrusion and cold compaction were theoretically investigated. SSPR involves densification of metallic alloy powders in temperature ranges when both solid and liquid phase coexist. The densification behavior of a composite strip by SSPR also has some differences compared with that of cold compaction, hot extrusion and liquid phase sintering. Besides, SSPR is a novel manufacturing technology of energy and material saving for strips. The study of densification process during SSPR can be of great importance in the further development of SSPR. The densification behavior of composite powders during rolling under semi-solid state is firstly discussed in this work. The densification process at different liquid fractions during semi-solid powder rolling is also firstly analyzed. Lastly, the relationship between deformation and densification is analyzed.

2 Experimental

A schematic of the approach and the actual experimental apparatus are shown in Fig. 1. The mixed powders used in this work are the gas-atomized 2024 aluminum alloy powders (Al−4.09Cu−1.18Mg−0.54Mg−0.21Fe) and the B_4C powders with the mean particle diameter of 25 μm. The AA2024 powders are nearly spherical and the mean particle diameter is 75 μm. The experiments were carried out on a powder rolling machine with rollers pre-heated to 300 °C. The diameter of roller is 150 mm with a width of 100 mm and a rotating speed of 0.4 rad/s. The mixed powders were firstly heated to 550, 585, 605, 625 °C, respectively and held for 30 min and then fed into the gap to produce strips with a width of 100 mm and a thickness of 2.5 mm to 3 mm.

In order to measure the rolling force during SSPR, a NIUSB data acquisition (DAQ) device (800392c−01) NI−9317 by National Instruments was used. The location of load sensor is shown in Fig. 1(b). The relative densities under different rolling forces were obtained by adjusting the rolling gap (the rolling gaps are 0, 0.5, 1.0, 1.5, 2.0, 2.5 mm, respectively). Afterward, the relative density of each sample was tested according to Archimedes principle. Wax was evenly coated on the surface of every sample in order to prevent the water going into the pores of the sample. The microstructures of etched samples were observed with an optical microscope (Lei-ca DMI500M). The SEM observation was carried out on NovaNanoSEM430 for identifying the morphology and distribution of second phase particles. The tensile test was carried out on SANS CMT5105 micro-computer control universal testing machine, and the test speed was 0.1 mm/min.

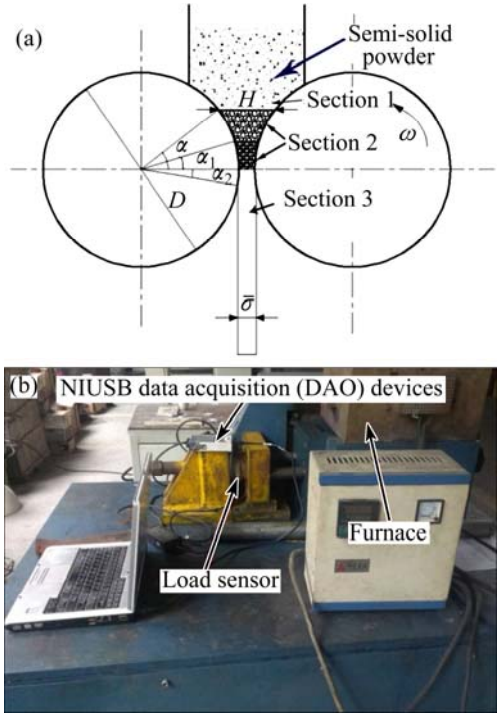

Fig. 1 Schematic of semi-solid powder rolling process (a) and experimental apparatus (b)

3 Results and discussion

3.1 Densification process during semi-solid powder rolling

Figure 2 shows the microstructures of strips heated at 605 °C for 30 min. Figure 2(a) shows that soft AA2024 matrix powder and hard B_4C particles stack loosely when the rolling force is 4.32 kN (the rolling gap is 2.5 mm). Many gap pores are observed. Most of mixed powders still remain the original morphology, which indicates that serious deformation does not take place on those powders. Experiments indicate that the strip cannot form when the rolling force is less than 4.32 kN (the rolling gap is more than 2.5 mm). The number of pores in the microstructure decreases obviously when the rolling force increases to 7.05 kN (the rolling gap is 2.0 mm). The prior particle boundaries of powders is still visible clearly, as shown in Fig. 2(b). As the rolling force increases to 11.7 kN (the rolling gap is 1.5 mm), a part of powders break up into smaller powders and others still keep their original morphology. The prior particle boundaries are still observed clearly, as shown in Fig. 2(c). The relative density of the strips increases obviously when the rolling force increases to 17.79 kN (the rolling gap is 1.0 mm). The primary reason of this phenomenon is that the elastic-plastic deformation occurs when the mixed powders are squeezed by the

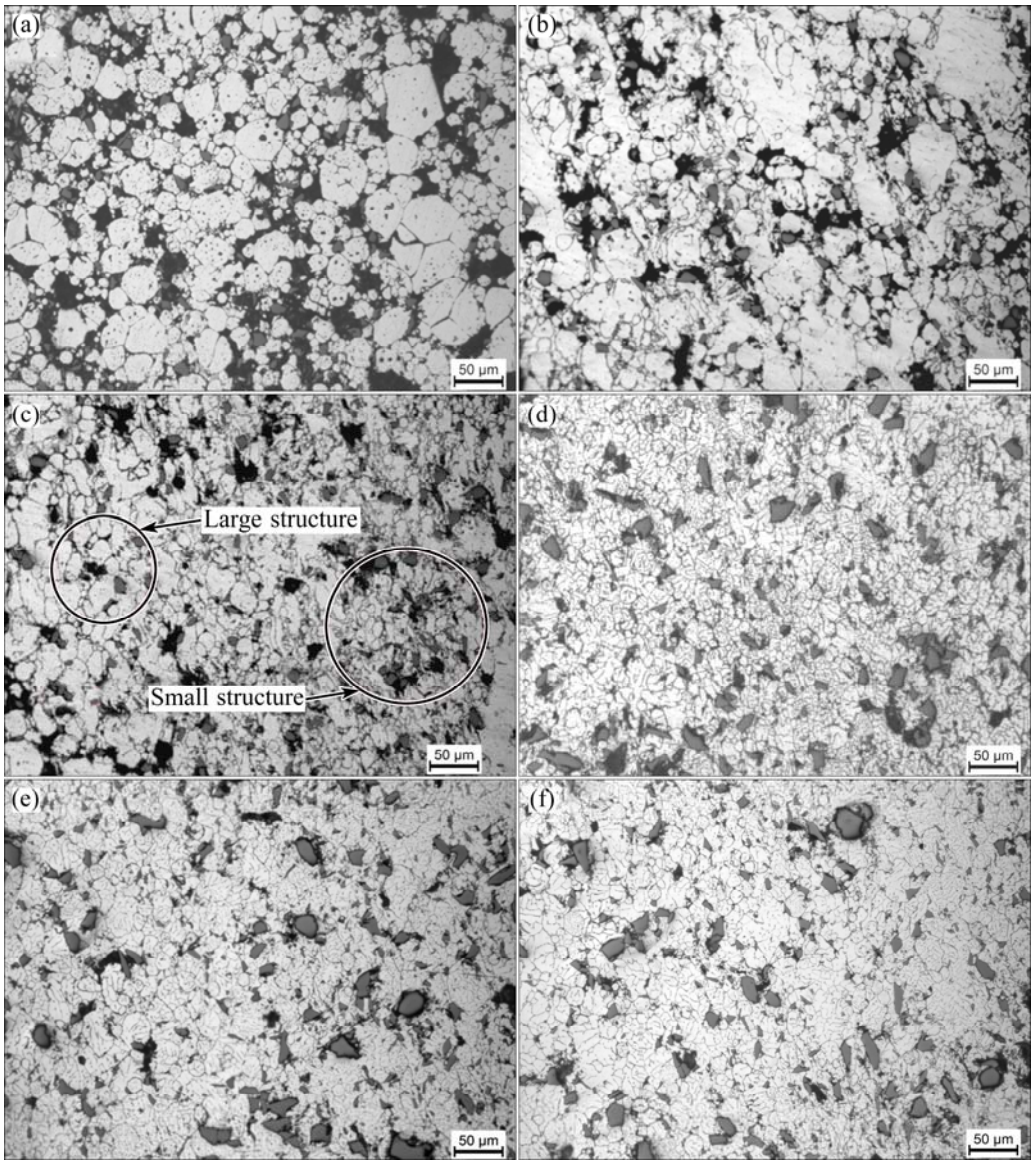

Fig. 2 Microstructures of strips heated at 605 °C for 30 min under different rolling forces: (a) 4.32 kN; (b) 7.05 kN; (c) 11.7 kN; (d) 17.79 kN; (e) 21.56 kN; (f) 24.31 kN

rolling force. Matrix powders break up when the rolling force exceeds the yield limit. The phenomenon can be explained by the rolling force changes in the curves shown in Fig. 3. As is detected, the rolling force curves look like a wavy line, which indicates that powders breakage and rearrangement occur during the whole process. It has been proved by many experiments that, the relative density of the strip increases sharply when the rolling force is more than or equal to 17.79 kN (the rolling gap is less than or equal to 1.0 mm), as shown in Figs. 2(d), (e) and (f).

In general, a finer grain size can be obtained as the rolling force increases during SSPR. The larger the rolling force is, the finer the microstructures are. More internal crystal lattice distortion can be gathered during powders breaking process, which results in a higher

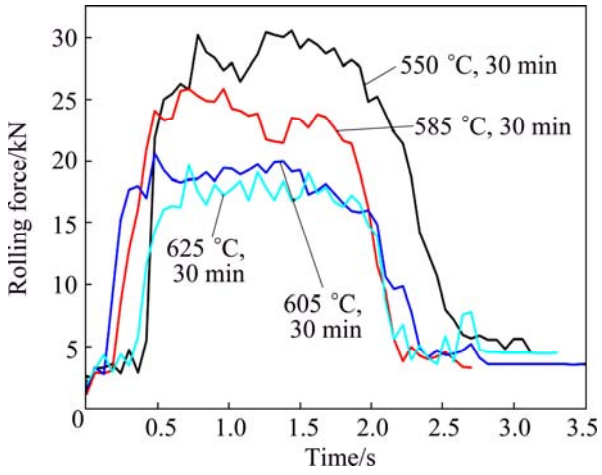

Fig. 3 Rolling force curves of B_4C−AA2024 composite strips by SSPR with rolling gap of 1.0 mm

dislocation density [10]. The difference between coefficients of thermal expansion (α) of the matrix and particle (α_{AA2024} is 22.8×10^{-6} K^{-1} and α_{B_4C} is 4.4×10^{-6} K^{-1}) causes thermal stress which is easier to form at the interface with higher rolling force [11,12]. The new dislocation accumulation generates at the barriers-particles when the thermal stress reaches a certain value [13]. Then, stress relaxation occurs, which increases the dislocation density. Smaller grains recreate subsequently.

The rolling force always changes during SSPR, as shown in Fig. 3. Apparently, the rolling force decreases with increasing temperature. The rolling force of a B_4C−AA2024 composite strip by SSPR is about 30 kN at 550 °C (the rolling gap is 1.0 mm). However, the rolling force decreases to about 17 kN when the temperature increases to 625 °C. This is because liquid phase plays an important role in forming a strip prepared by SSPR. Powders with high liquid fraction usually need a low force to deform or break up. The liquid fraction can be calculated by Scheil equation. The corresponding liquid fraction is summarized in Table 1. The liquid fraction is less than 10% at 550 °C, and the liquid fraction is as high as 56% at 625 °C. NEAG et al [14] stated that the powder with a high liquid phase can reduce the deformation resistance. As the temperature increases, the liquid fraction increases accordingly. Liquid phase forms a network when the liquid fraction is more than 20%, which can be squeezed out during rolling. The liquid phase flows among the powders, which not only reduces the flowing resistance of powders, but also reduces the deformation resistance of powders. Therefore, a high temperature contributes to densification during SSPR.

Table 1 Liquid fraction of 2024 aluminum alloy at different temperatures

Temperature/°C	Liquid fraction/%
550	5.93
585	13.15
605	40.16
625	56.03

The relative density of B_4C−AA2024 composite strips increases with the increase of temperature. The relative density is usually high with a high temperature when the rolling force remains constant. As shown in Fig. 4, the increase of relative density is slow when the temperature ranges from 550 to 585 °C.

The relative densities of all strips by SSPR are higher than 70%, which is higher than that of powder rolling (the relative density usually less than 70%). This is due to powders in semi-solid state which contain some liquid phases. It is an advantage of SSPR compared with powder rolling. The relative densities increase sharply when the temperature ranges from 585 to 625 °C (the liquid fraction ranges from 13.15% to 56.03%). KIM [15] stated that the liquid phase has a stronger influence on the densification of the materials. The liquid phase is isolated within the particle when the liquid fraction is lower than 20%. The liquid phase forms a network when liquid fraction is equal to or higher than 20%, as shown in Fig. 5. So, the reason for the relative densities increasing sharply from 585 to 625 °C is that some liquid phase can be squeezed out during rolling, which may fill in the pores between powders.

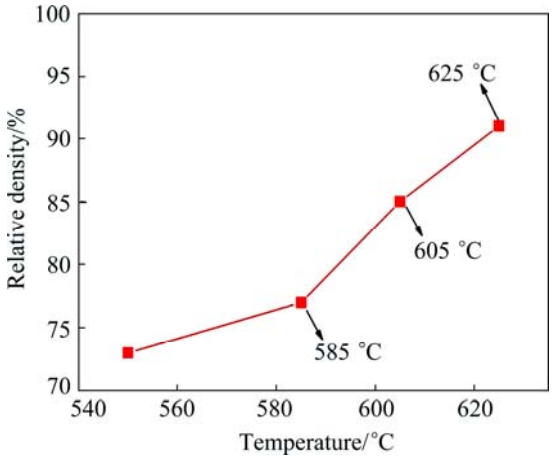

Fig. 4 Curves of relative density and temperature for B_4C−AA2024 composite strips at rolling gap of 1.0 mm

Although the strips can be formed at 550 °C and 585 °C, there are still many pores located among the tri-boundaries of particles (Figs. 6(a) and (b)). As mentioned above, there is no liquid to fill into the pores at 550 °C and 585 °C, which leads to a low relative density. When the temperature increases to 605 °C and 625 °C, the relative density of strips by SSPR is higher than 0.85. This is because many liquid phases are squeezed out and then fill into the pores, which results in the increase of relative density, as shown in Figs. 6(c) and (d).

3.2 Densification mechanism during semi-solid powder rolling

Various stages of densification process are schematically shown in Fig. 7 for an idealized case. The densification process can be divided into three stages. As shown in Stage 1, in the feeding area, the AA2024 powders and B_4C particles rearrange and restack randomly without deformation. The powders are still in semi-solid state. The irregular solid phase and B_4C particles can be regarded as a skeleton. Isolated liquid phase is observed when the liquid fraction is less than 20%, as shown in Fig. 8(a) (the powder was heated at 550 °C for 30 min). Liquid networks form when liquid fraction is higher than 20%, as shown in Fig. 8(b) (the

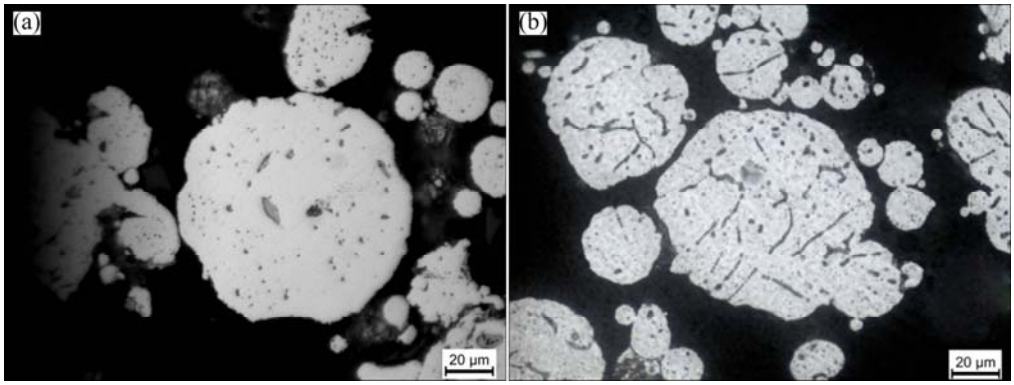

Fig. 5 Microstructures of semi-solid powders heated at different temperatures: (a) 585 °C, 30 min; (b) 625 °C, 30 min

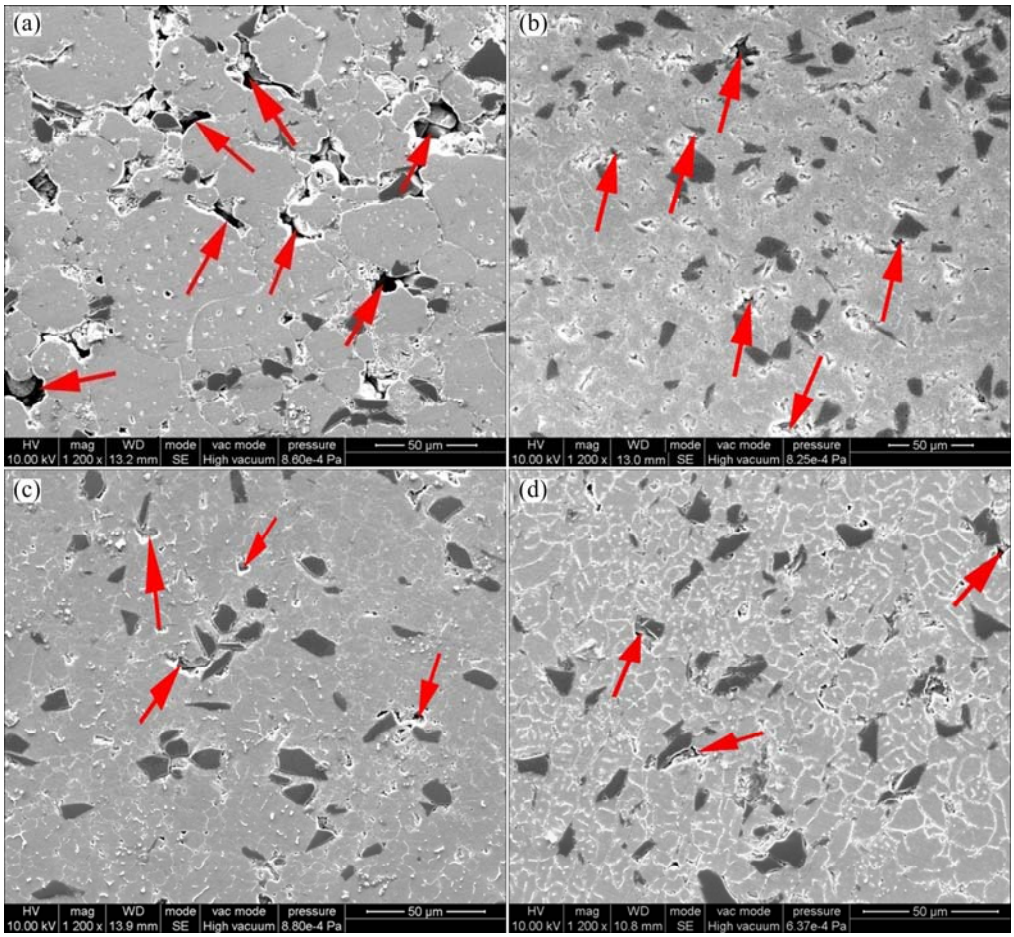

Fig. 6 SEM images of B_4C−AA2024 composite strips prepared under different temperatures with rolling gap of 1.0 mm: (a) 550 °C, 30 min; (b) 585 °C, 30 min; (c) 605 °C, 30 min; (d) 625 °C, 30 min

powder was heated at 625 °C for 30 min). So, the densification mechanism can be divided into two situations. The first situation is that the liquid fraction is less than 20%, another is equal to or higher than 20%, as shown in Fig. 8. In Stage 1, the loose powders have the dominant densification mechanism of rearrangement by sliding between powders.

In Stage 2, in deformation area, the rolling force on the powders increases accordingly with rolling. The powders start to deform along the rolling direction. Then, powders break up when the rolling force on the powders exceeds the yield limit of powders. The broken powders are easier to flow and fill into the gaps among powders due to their smaller volume, which result in the reduction or disappearance of the pores. When the liquid fraction is less than 20%, the deformation resistance of powders is very large. A lot of distortion energy gathers in powder during the breaking process, which results in the increase

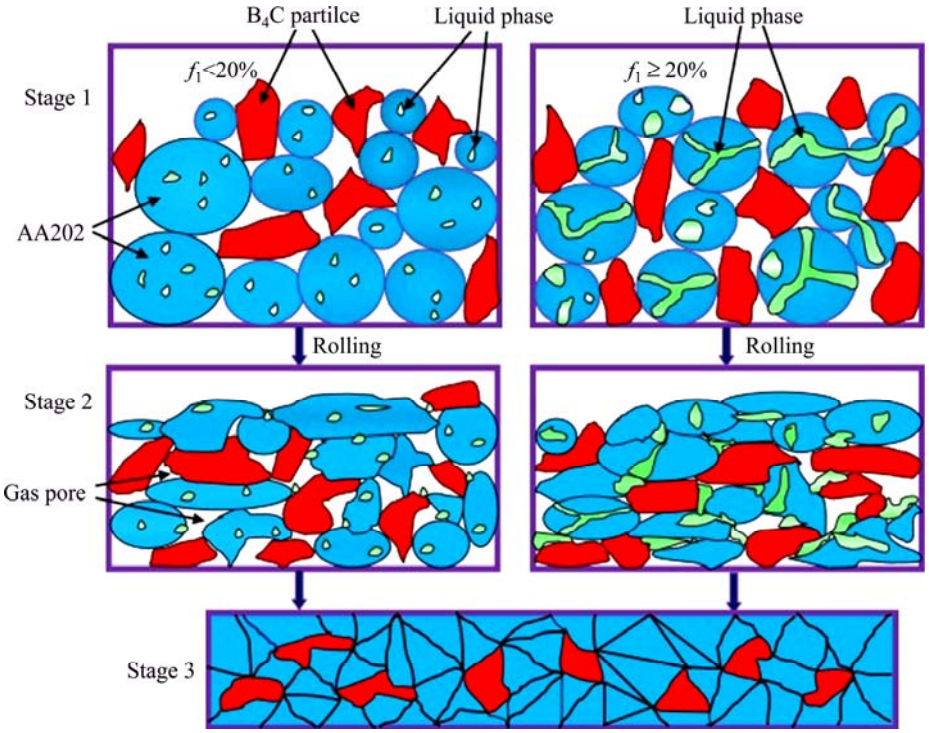

Fig. 7 Schematic diagram of semi-solid powder rolling

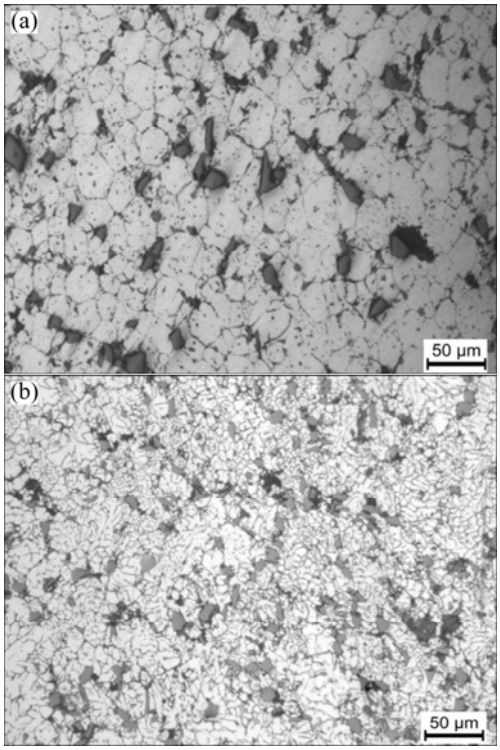

Fig. 8 Microstructures of different liquid fractions (f_l): (a) f_l<20%; (b) f_l≥20%

of temperature of powders [16]. Then, metallurgical bonding occurs among powders. When the liquid fraction is equal to or higher than 20%, the deformation resistance of powder is small. Powders are easy to deform and break up. The liquid phases in the powders can be squeezed out. In short, in the deformation area, the metallurgical bonding of powders is the main densification mechanism when the liquid fraction is less than 20%. The filling and flowing of liquid are the main densification mechanisms when the liquid fraction is equal to or higher than 20%.

KIM [15] developed a unified densification model based on the micro-mechanics framework for porous plastic materials in order to further explain the densification behavior of composite, these equations are as follows:

$$\dot{\bar{\varepsilon}}_p = \frac{\alpha}{d\gamma}\sinh[\beta(\bar{\sigma} - X - \bar{\sigma}_y)] \quad (1)$$

$$\dot{X} = (C_1 - \gamma_1 X)\dot{p} \quad (2)$$

$$\dot{d} = \frac{\alpha_1 + \beta_1 \dot{\bar{\varepsilon}}_p}{d^{\mu}} \quad (3)$$

where $\dot{\bar{\varepsilon}}_p$ is the plastic strain rate, $\bar{\sigma}$ is the true stress, X is the internal stress, $\bar{\sigma}_y$ is the yield stress, $\dot{p}$ is the effective plastic strain rate, d is the mean grain size, and α, β, γ, γ_1, α_1, β_1, C_1 and μ are material-dependent parameters. In order to determine the deformation behavior of matrix materials and the parameters, the stress−strain behaviors of the strips were measured through experiment.

The engineering stress and the strain increase with increasing temperature, as shown in Fig. 9. However, it could be noted that the stresses of the composites do not

show any sharp yield point. All the stresses do not follow any specific trend with strain rate. The difference of stress between 550 °C and 625 °C is obvious. The engineering stress here is about 80 MPa at 550 °C and 170 MPa at 625 °C. As shown in the former discussion, the liquid phase flows and fills in the pores or channels until the pores or channels disappear at 625 °C (the liquid fraction is about 60%), which results in the increase of tensile strength. Due to no liquid flowing and filling in the pores at 550 °C, the materials have many pores at last, which result in lower tensile strength and relative density, Fig. 6 is the proof.

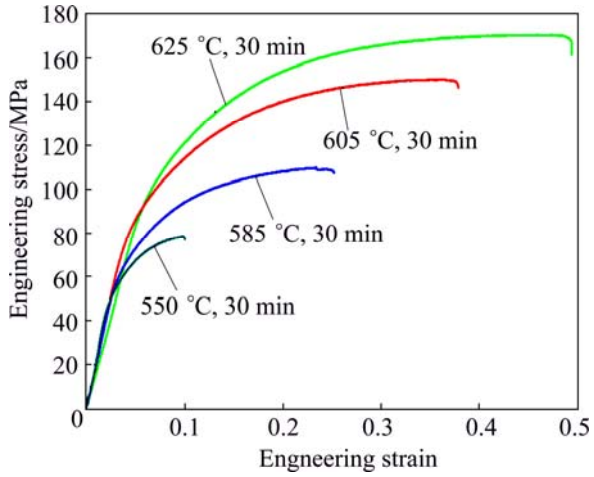

Fig. 9 Measured engineering stress−strain curves of B_4C−AA2024 samples with same rolling gap of 1.0 mm

In Stage 3, a dense composite strip by semi-solid powder rolling is obtained. Aggregation of B_4C particles is not observed in any particular region. The B_4C particles are distributed uniformly in AA2024 matrix which contributed to transferring loading from matrix to reinforcement.

3.3 Relationship between relative density and rolling force

The relative density of B_4C−AA2024 composite strips increases with the increase of the rolling force. Apparently, a higher rolling force is required at a lower temperature, as shown in Fig. 10. The increase of relative density is slow when the rolling force is less than the yield limit of powders. Many powders may show elastic deformation rather than breakage. LIU et al [4] used Shima−Oyane model to predict the relative density distribution during semi-solid powder rolling when the liquid fraction is lower than 20%. Similarly, Shima−Oyane model also goes for mixed powders of composite with a low liquid fraction. As the curves shown in Figs. 10(a) and (b), the relative density–rolling force curves are similar to each other at 550 °C and 585 °C (the liquid fraction is 5.93% and 13.15%, respectively). WU and KIM [7] stated that the overall deformation mechanism of Al6061 in the semi-solid region at low liquid fraction was consistent. In order to confirm the accuracy of the model, additional six samples were prepared at different rolling forces and 550 °C. The results show that the additional curve shape at 550 °C is almost identical with that of the curves at 550 °C, which is enough to prove that the Shima−Oyane model is fit for semi-solid mixed powders with a liquid fraction lower than 20%. Based on the former discussion, higher rolling force applied on the powders contributes to the deformation. Therefore, large extent of deformation in powders is helpful for the improvement of relative density.

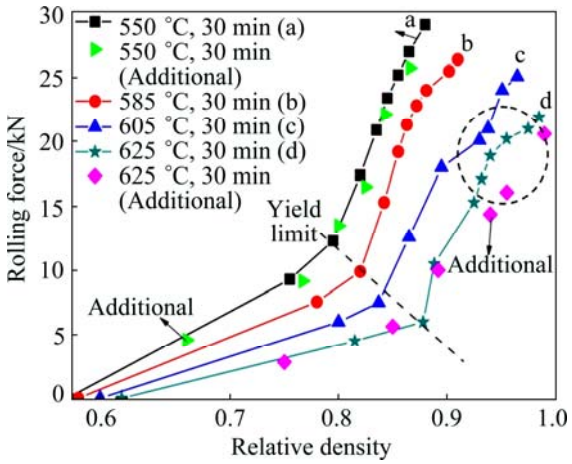

Fig. 10 Curves of rolling force and relative density for B_4C−AA2024 composite strips at different temperatures

Shima−Oyane model which is based on the hot rolling of porous strip cannot be acceptable when the liquid fraction is equal to or higher than 20%. This is because an amount of liquid phase is squeezed out. The liquid phase flows and fills among powders, resulting in the change of the structural deformation property. The characteristics of the curve shape are different at 605 °C and 625 °C (the liquid fraction is 40.16% and 56.03%, respectively), as shown in Figs. 10(c) and (d). An apparent difference of rolling force and relative density is observed at the round box. Similarly, the same method was used to confirm the point. Additional six samples were prepared at varying rolling force and 625 °C. The curve shapes of additional samples at 625 °C are apparently different from those at 625 °C, which is caused by randomness of the liquid flowing. Therefore, Shima−Oyane model fails to predict the densification behavior when the liquid fraction is equal to or higher than 20%. In short, with a higher liquid fraction, the liquid phase is squeezed out during the rolling. The liquid phase flows and fills into the pores, resulting in the improvement of the strength and the relative density of materials.

4 Conclusions

1) Semi-solid powder rolling (SSPR) can be used to prepare composite strips. Particle rearrangement and restack are the densification mechanisms in feeding area. When the liquid phase is lower than 20%, rolling deformation is the main densification mechanism in deformation area. When the liquid fraction is higher than 20%, the flowing and filling of liquid are the densification mechanisms.

2) A finer grain size can be obtained with increasing rolling force. Higher rolling force is required for the rolling of powders with lower temperature. When the rolling force is constant, the relative density is usually high at a high temperature.

3) Shima−Oyane model goes for mixed powders of composite when the liquid fraction is lower than 20%. Shima−Oyane model fails to predict the density change when the liquid fraction is equal to or higher than 20%.

References

[1] LIU Bin, HUANG Wen-mao, WANG Hao-wei, WANG Ming-liang, LI Xian-feng. Compressive behavior of high particle content B_4C/Al composite at elevated temperature [J]. Transactions of Nonferrous Metals Society of China, 2013, 23(10): 2826−2832.

[2] NIE Cun-zhu, GU Jia-jun, LIU Jun-liang, ZHANG Di. Investigation on microstructures and interface character of B_4C particles reinforced 2024Al matrix composites fabricated by mechanical alloying [J]. Journal of Alloys and Compounds, 2008, 454: 118−122.

[3] TOPCU I, GULSOY H O, KADIOGLU N, GULLUOGLU A N. Processing and mechanical properties of B_4C reinforced Al matrix composites [J]. Journal of Alloys and Compounds, 2009, 482(1−2): 516−521.

[4] LIU Yun-zhong, LUO Xia, LI Zhi-long. Microstructure evolution during semi-solid powder rolling and post-treatment of 7050 aluminum alloy strips [J]. Journal of Materials Processing Technology, 2014, 214: 165−174.

[5] ATKINSON H V, LIU D. Coarsening rate of microstructure in semi-solid aluminium alloys [J]. Transactions of Nonferrous Metals Society of China, 2010, 20(9): 1672−1676.

[6] LANGE F F, ATTERAAS L, ZOK F, PORTER J R. Deformation consolidation of metal powders containing steel inclusions [J]. Acta Metallurgica et Materialia, 1991, 39(2): 209−219.

[7] WU Yu-feng, KIM G Y. Compaction behavior of Al6061 powder in the semi-solid state [J]. Powder Technology, 2011, 214: 252−258.

[8] KIM K T, CHO J H, KIM J S. Cold compaction of composite powders [J]. Journal of Engineering Materials and Technology, 2000, 122(1): 119−128.

[9] BORSA C E, FERREIRA H S, KIMINAMI R H G A. Liquid phase sintering of Al_2O_3/SiC nanocomposites [J]. Journal of the European Ceramic Society, 1999, 19(5): 615−621.

[10] HAGHDADI N, ZAREI-HANZAKI A, HESHMATI-MANESH S, ABEDI H R, HASSAS-IRANI S B. The semisolid microstructural evolution of a severely deformed A356 aluminium alloy [J]. Materials and Design, 2013, 49: 878−887.

[11] WU Yu-feng, KIM G Y, ANDERSON I E, LOGRASSO T A. Fabrication of Al6061 composite with high SiC particle loading by semi-solid powder processing [J]. Acta Materialia, 2010, 58: 4398−4405.

[12] YANDOUZI M, BOTTGER A J, HENDRIKX R W A, BROCHU M, RICHER P, CHAREST A, JODOIN B. Microstructure and mechanical properties of B_4C reinforced Al-based matrix composite coatings deposited by CGDS and PGDS processes [J]. Surface & Coatings Technology, 2010, 205: 2234−2246.

[13] DURISINOVA K, DURISIN J, OROLINOVA M, DURISIN M. Effect of particle additions on microstructure evolution of aluminum matrix composite [J]. Journal of Alloys and Compounds, 2012, 525: 137−142.

[14] NEAG A, FAVIER V, BIGOT R, POP M. Microstructure and flow behavior during backward extrusion of semi-solid 7075 aluminium alloy [J]. Journal of Materials Processing Technology, 2012, 212: 1472−1480.

[15] KIM T W. Determination of densification behavior of Al−SiC metal matrix composites during consolidation processes [J]. Materials Science and Engineering A, 2008, 483−484: 648−651.

[16] ZHENG Rui-xiao, CHEN Jing, ZHANG Yi-tan, AMEYAMA K, MA Chao-li. Fabrication and characterization of hybrid structured Al alloy matrix composites reinforced by high volume fraction of B_4C particles [J]. Materials Science and Engineering A, 2014, 601: 20−28.

半固态粉末轧制法制备 10%B_4C−AA2024 复合材料带材的致密化过程

莫灼强，刘允中，贾惠芳，吴 敏

华南理工大学 国家金属材料近净成形工程技术研究中心，广州 510640

摘 要：半固态粉末轧制法是一种制备带材的新型工艺方法，既包含有粉末轧制技术的优点，也包含有半固态轧制技术的优点。研究 B_4C 与 AA2024 混合粉末颗粒在存在液相情况下的致密化过程和变形规律，同时分析相对密度与轧制力的关系。结果表明，液相分数对半固态粉末轧制带材的致密化过程有着重要的影响。致密化过程可分为 3 个阶段。当液相分数低于 20%时，轧制变形成为主要的致密机制；当液相分数高于 20%时，液相的流动与填充成为带材的致密机制。随着轧制力的增加，材料相对密度增大。在 550 °C 和 585 °C 条件下得到的相对密度与轧制力曲线变化趋势相一致。而 605 °C 和 625 °C 得到的相对密度与轧制力曲线趋势明显不一致。

关键词：半固态粉末轧制；复合材料带材；致密过程；轧制变形

(Edited by Yun-bin HE)